Virus Research 274 (2019) 197777

Contents lists available at ScienceDirect

Virus Research

journal homepage: www.elsevier.com/locate/virusres

The activity of Aurora kinase B is required for dengue virus release

J. Humberto Pérez-Olais[a], Fernando Ruiz-Jiménez[b], Esther J. Calderón-Garcia[a], L. Adrián De Jesús-González[a], Rosaura Hernández-Rivas[c], Rosa M. del Angel[a,*]

[a] Infectomics and Molecular Pathogenesis Department, Center for Research and Advanced Studies-IPN, Mexico City, Mexico
[b] Molecular Virology, School of life Sciences, The Nottingham University, Nottingham, UK
[c] Molecular Biomedicine Department, Center for Research and Advanced Studies- IPN, Mexico City, Mexico

ARTICLE INFO

Keywords:
Kinases
Dengue virus
Aurora kinase B
Viral release

ABSTRACT

Flaviviruses, such as Dengue (DENV), Zika, Yellow Fever, Japanese Encephalitis and West Nile are important pathogens with high morbidity and mortality. The last estimation indicates that ~390 millions of people are infected by DENV per year. The DENV replicative cycle occurs mainly in the cytoplasm of the infected cells and different cytoplasmic, nuclear and mitochondrial proteins participate in viral replication. In this paper we analyzed the participation of Aurora kinase B (AurKB) in the DENV replicative cycle using the specific AurKB inhibitor ZM 447439. The kinase inhibition does not alter the viral protein production/secretion or genome replication but impaired the viral yield without altering the percentage of infected cells. Moreover, confocal microscopy analysis of DENV-infected ZM 447439-treated cells show a delocalization of viral components from the replicative complexes. In summary, these observations indicate that AurKB participates in DENV viral morphogenesis or release.

1. Introduction

In the last years, the emergence of different arboviruses has generated a global health alert. Among arboviruses, Dengue (DENV), is one of the most prevalent arboviruses in the world and it is the causative agent of approximately 390 millions of infections per year. The World Health Organization calculates that half of world population (3.6 billion of persons) is at risk of infection with any of the four DENV serotypes (WHO, 2009; Bhatt, Gething et al. 2013), being *Aedes aegypti* and *A. albopictus,* the main vectors for DENV, both highly adapted to the urban environment (Suwonkerd, Mongkalangoon et al. 2006). DENV can cause a symptomatic febrile illness called dengue fever (DF) that can evolve to a more severe form of the disease known as severe dengue characterized by plasma leakage. Given the recent complications in the guidelines for vaccination with Dengvaxia® (Sanofi, 2017) and the lack of an approved antiviral drug, it is necessary to identify potential new targets against DENV infection.

DENV genome is a single strand of positive polarity RNA of about 11 kb with a unique open reading frame which encodes a polyprotein cleaved co- and post-translation by viral and cellular proteases to generate three structural (C, prM/M and E) and seven non-structural (NS1, NS2A, NS2B, NS3, NS4A, NS4B and NS5) proteins (Lindenbach and Rice, 2003). The replicative cycle of DENV takes place in the cytosol, mainly in the endoplasmic reticulum (ER). In this place, the DENV non-structural proteins induce invaginations in the ER membranes to form the replicative complexes (RCs) connected with the cytosol via pores allowing the exit of viral RNA for DENV assembly (Miller, Sparacio et al. 2006; Welsch, Miller et al. 2009; Harak and Lohmann, 2015). Viral morphogenesis also occurs in ER vesicles near to the RCs being the endosomal sorting complex required for transport III (ESCRT-III) activity necessary for effective viral release from the ER to Golgi cisternae. The subunit CHMP4 A–C from ESCRT has been described as necessary for flavivirus viral morphogenesis and budding (Tabata, Arimoto et al. 2016). Finally, in the Golgi apparatus, the furin protease cleaves the pr peptide from prM allowing viral maturation through the secretory pathway (Murray, Aaskov et al. 1993).

Viruses, as intracellular obligate parasites, hijack cellular proteins, components and processes to be replicated in the host cell. Thus, the identification of host proteins involved in viral replicative cycle is relevant to recognize new host targets to control DENV infection or progression to severe clinic forms.

Protein kinases regulate several cellular processes such as energy production, cellular growth, cell cycle, and interferon signaling, among others. It has been described that the activity of some protein kinases is

* Corresponding author.
E-mail addresses: jholais@gmail.com (J.H. Pérez-Olais), ferrj2510@gmail.com (F. Ruiz-Jiménez), ejcalderon@outlook.com (E.J. Calderón-Garcia), luis.dejesus@cinvestav.mx (L.A. De Jesús-González), rohernan@cinvestav.mx (R. Hernández-Rivas), rmangel@cinvestav.mx (R.M. del Angel).

https://doi.org/10.1016/j.virusres.2019.197777
Received 24 May 2019; Received in revised form 11 September 2019; Accepted 7 October 2019
Available online 15 October 2019
0168-1702/

required for viral entry, assembly, and release (Anwar, Hosoya et al. 2011; Keating, Bhattacharya et al. 2013; Bekerman, Neveu et al. 2017). Specifically, the inhibition of the Epidermal grow factor receptor (EGFR) kinase, the AMP dependent kinase (AMPK), the AP-2 Associated protein kinase (AAK1), and the Cyclin G Associated Kinase (GAK) induces an inhibition in Yellow fever virus (YFV), Japanese encephalitis virus (JVE), and DENV replication (Kovackova, Chang et al. 2015; Madejon, Sheldon et al. 2015; Jordan and Randall, 2017; Limjindaporn, Panaampon et al. 2017).

Aurora kinases A, B, and C are members of the serine/threonine aurora kinase family and are considered as master regulators of the cell cycle. In particular, Aurora kinase B (AurKB) forms a complex with Inner Centromere Protein (INCENP), borealin, and survivin to constitute the chromosomal passenger complex (CPC)(Carmena, Wheelock et al. 2012). The main role of this complex is the correct chromosome segregation and cytokinesis. During the cytokinesis the *CPC* interacts through AurKB with the ESCRT-III subunit, Charged Multivesicular Body Protein 4C (CHMP4C), which has been described that is required for flavivirus budding from endoplasmic reticulum (Tabata, Arimoto et al. 2016). It has also been described that AurKB is involved in the replicative cycle of several other viruses such as Epstein Barr virus, favoring B cells proliferation and transformation mediated by the p53 regulation, for influenza virus replication and for Hepatitis C virus (HCV) viral particle production (Jha, Lu et al. 2013; Jha, Yang et al. 2015; Madejon, Sheldon et al. 2015; Hu, Zhang et al. 2017).

In the present work, we analyzed the role of AurKB during DENV 2 infection using the specific AurKB inhibitor ZM 447439 (Georgieva, Koychev et al. 2010). The inhibition of AurKB induced a reduction in viral particle production without an alteration in viral translation and replication. Moreover, the RCs distribution was clearly altered after treatment with the inhibitor ZM 447439. A similar effect was detected after AurKB silencing. All these results indicate that AurKB kinase activity is required for DENV morphogenesis and/or release.

2. Material and methods

2.1. Cell line and viruses

Huh-7 cells, a differentiated hepatocyte derived cellular carcinoma cell line (kindly donated by Dr. Rivas from Universidad Autónoma de Nuevo Leon) were cultured in advanced DMEM supplemented with 2 mM glutamine, penicillin (5×10^4 U/ml)-streptomycin (50 µg/ml), 5% fetal calf serum (FCS), and 1 ml/l of amphotericin B (Fungizone) at 37 °C in a 5% CO2 humidified atmosphere. The DENV propagation, serotype 2 New Guinea strain was carried out in CD1 suckling mice brains (provided by Unidad de Producción y Experimentación de Animales de Laboratorio (UPEAL).

2.2. Drug and antibodies

The AurKB inhibitor ZM 4474389 synthetized by Astra-Zeneca was provided by *Tocris BioScience* and was dissolved in DMSO (Vehicle) to prepare a stock solution at 9 mM. The follow primary antibodies were used: α-NS3 (GTX124252), α-Env 4G2 clone Hb 119, α-prM-E 2H2, α-dsRNA (kindly donated by Dr. Mariano Garcia-Blanco) and α-capside antibodies (kindly donated by Dr. Andrea Gamarnik).

2.3. Metabolic and cell viability analysis

Huh-7 cells were seeded in 96 well/plate, after 24 h, the cells were treated with vehicle (DMSO 0.11%) or with different concentrations of ZM 447439 for 24 h. Later, cell metabolism was evaluated by the MTS reduction using Cell Titer 96 Aqueous One Solution Reagent (Promega) following the manufacturer's protocol. In parallel, a flow cytometry assay was performed to analyze cell viability through the propidium iodide (PI) uptake.

2.4. DENV infection and ZM 447439 treatment

Briefly, the cells Huh-7 at ~80% confluence were washed with PBS or Hanks medium three times and were infected with DENV at a MOI of 3 diluted in DMEM supplemented with 1% of FBS. The infection was permitted for 2 h at 37 °C. Later, cells were treated with acid glycine (pH 3.0) to inactivate the non-internalized viral particles. Next, cells were washed three times with Hanks medium and incubated in complete medium with ZM 447439 for 24 and 48 h at 37 °C. Two different concentrations of ZM 447439 were used: 1 and 5 µM in complete medium.

2.5. Forming focus assay and NS1 secretion

The supernatants from cells infected and untreated or treated with ZM 447439 were collected. The NS1 secretion was measured in the supernatants using an ELISA kit following the manufacturer's protocol (Platelia, BioRad). For focus forming assay, confluent monolayers of Huh-7 cells grown in 96-well plates were inoculated with serial dilutions of the supernatant media from DENV infected cells (final volume 50 µl) for 1 h at 37 °C to allow viral adsorption. Then, the inoculum was removed; cell monolayers were washed once with Hank's solution and 0.2 ml of complete media was added. The medium was removed at 48 h post infection (h.p.i.) and cells were fixed with 1% formaldehyde, permeabilized for 20 min, incubated with 2H2 monoclonal antibody overnight at 4 °C, and later with anti-mouse FITC secondary antibody for 2 h at room temperature (RT). Foci were observed by epi-fluorescence microscopy and expressed as Focus Forming Units (FFU)/ml.

2.6. Plaque forming assay

BHK-21 cells monolayers (2.5×10^5 cells at 90% confluence in 24-well plates) were infected with different dilutions of the supernatant from infected and silenced cells for 4 h at 37 °C. Overlay medium (0.5 mL; MEM supplemented with 7.5% FBS, 1% carboxymethylcellulose, and antibiotics) was then added, and the cells were incubated for five days at 37 °C in a 5% CO_2 humidified atmosphere. Finally, the medium was removed, and the monolayers were stained with naphthol blue black (0.1% naphthol blue black, 0.165 M sodium acetate, and 6% acetic acid) for 15 min at RT, and the viral yield from three independent experiments was measured and expressed in the log of plaque forming units (PFU)/ml.

2.7. Western blot analysis

Briefly, Huh-7 cells grown in 6 wells plate were infected with DENV and untreated or treated with ZM 447439 for 24 and 48 h.p.i. Then, cells were lysed with RIPA buffer in the presence of proteases and phosphatases inhibitors (Complete and PhosStop, Roche). The lysate was clarified by centrifugation and 40 µg of protein were separated by SDS-PAGE and immunoblotting using the proper primary antibody: anti-H3 (1:5000, abcam ab107799), anti-H3S10ph (1:5000, abcam ab14955), anti-NS3 (1:1000, Genetex GTX124252), or anti-AurKB (Invitrogen, 36–5200), β-actin was used as loading control. Anti-rabbit HRP, and anti-mouse HRP, (1:7000, Cell Signaling) were used as second antibodies in all cases. The proteins were visualized using Super Signal West Femto Chemiluminescent Substrate (Thermo Scientific). Densitometric analysis was performed using the ImageJ software (National Institutes of Health) and adjusted with the loading control (β actin).

2.8. Immunofluorescence assay

The Huh-7 cells grown on slides were infected with DENV 2 and 24 h.p.i. were fixed with 4% paraformaldehyde (PFA) for 20 min and

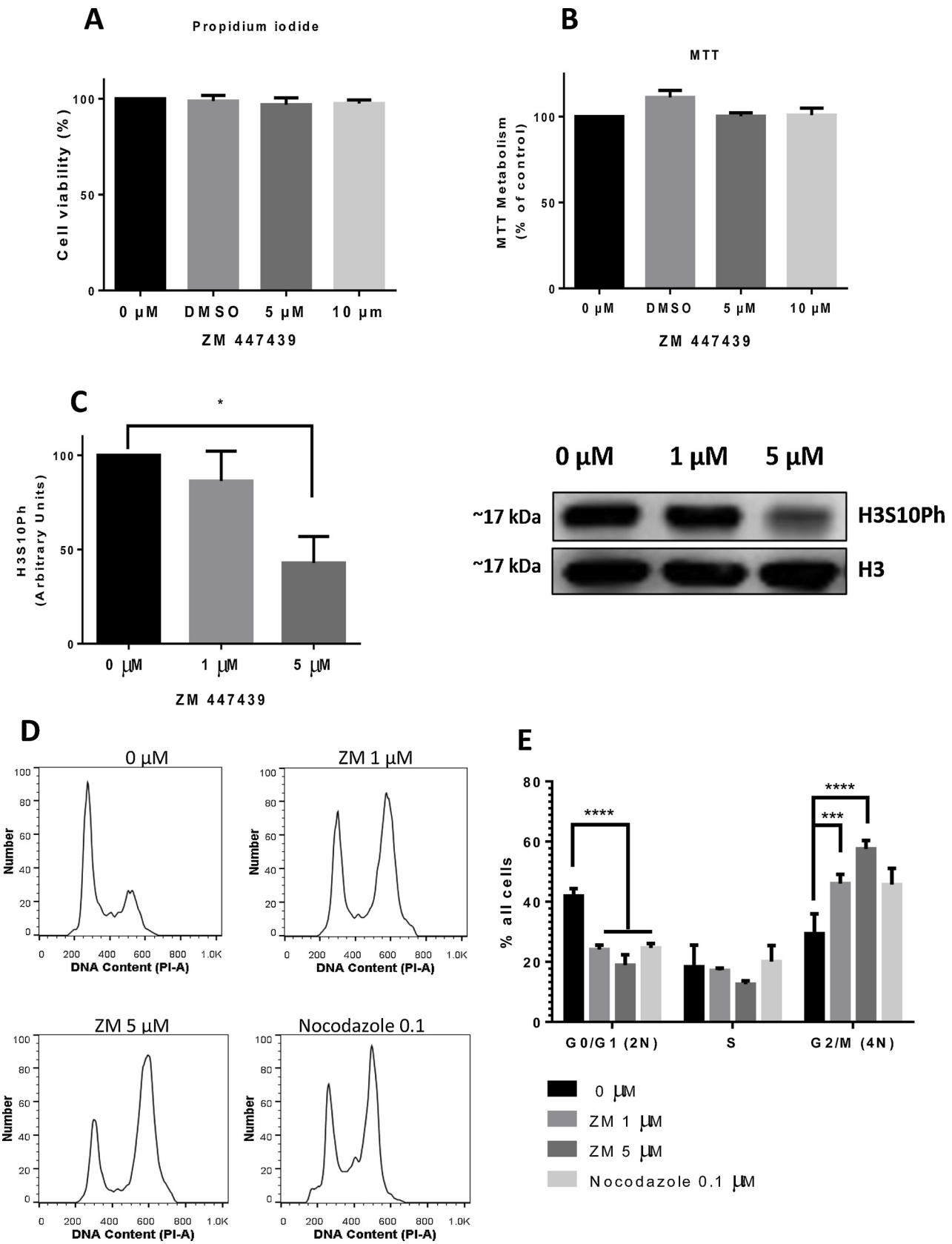

Fig. 1. ZM 447439 inhibits AurKB activity without any effect in cell viability. Huh-7 cells were treated with different concentration of ZM 447439 for 24 h and the cell viability and metabolism were measured by propidium iodide uptake (A) and MTS reduction assays (B). Graphs represent the relative quantification of cell viability respect to cells treated with 0 µM of ZM 447439. Data are means ± standard error (S.E) of three independent experiments $*p < 0.05$. (C) Huh-7 cells were treated with ZM 447439 at 1 and 5 µM for 24 h and the phosphorylation of H3 histone was analyzed by Western-blot assay using an anti-H3S10p antibody. Total H3 was used as a loading control. Data are means ± standard error (S.E) of three independent experiments. $*p < 0.05$ (D) The cell cycle arrest was observed by flow cytometry using Propidium iodide/RNase A staining buffer (D and E).Data are means ± standard error (S.E) of three independent experiments. $***p < 0.05$ and $****p < 0.001$.

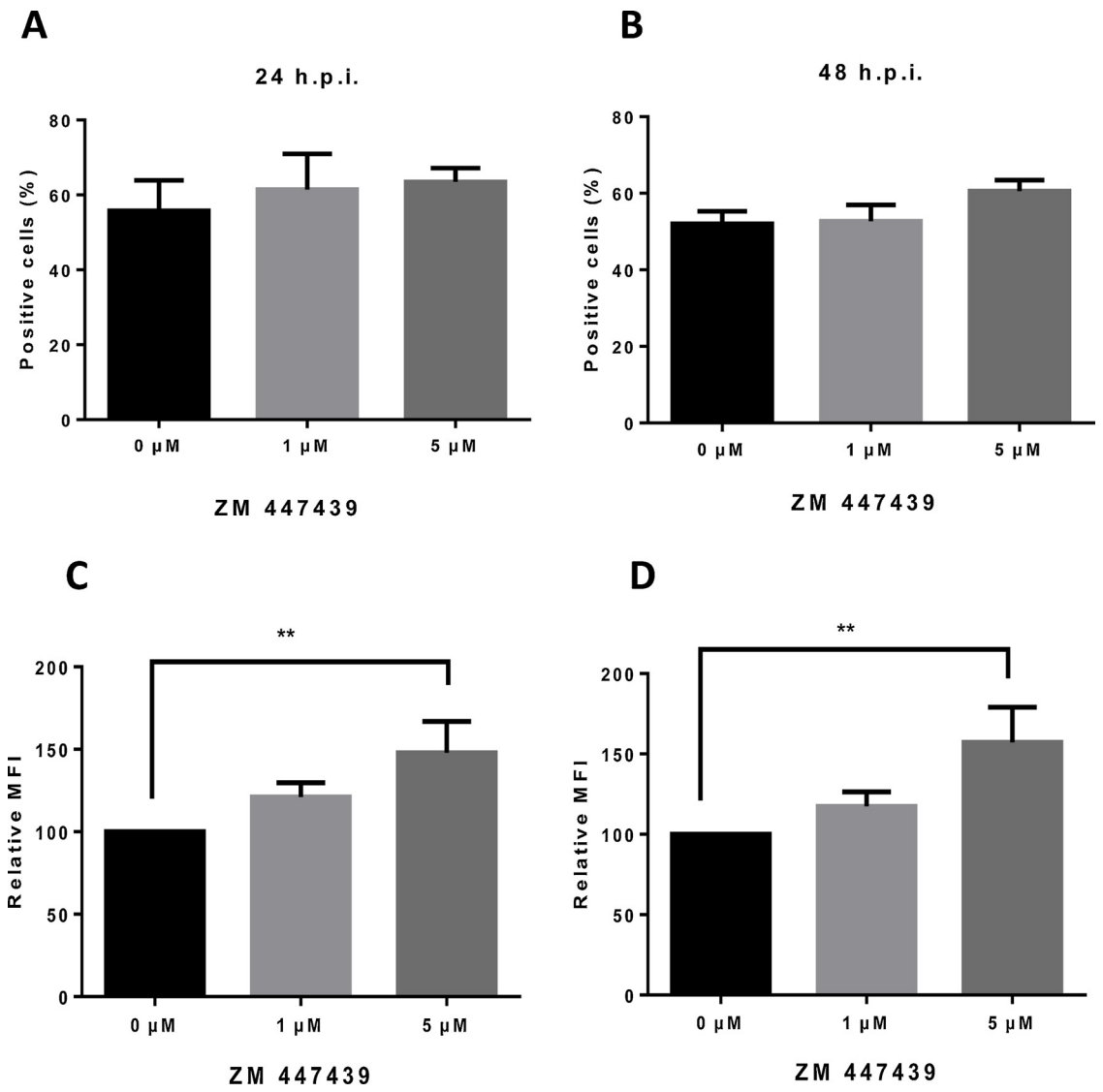

Fig. 2. Effect of ZM 447439 in DENV2 infection efficiency. Huh-7 cells infected at MOI of 3 were treated with 1 µM and 5 µm of ZM 447439 for 24 (A and C) or 48 h (B and D). The relative percentage of infected cells (A and B) and the relative mean fluorescence intensity (MFI) (C and D) were determined under the same conditions by flow cytometry. Graphs show mean ± SEM of three independent experiments. *P < 0.05.

permeabilized with PermWash solution (PBS 1X, FCS 1% and saponine 0.2%) for 20 min. Later, cells were incubated with the respective primary antibody overnight at 4 °C and with the secondary antibody for 2 h at RT. All antibodies were diluted in PermWash solution. The nuclei were stained with DAPI and the slices covered with VectaShield. Images were captured with Zeiss LSM700 laser confocal microscope and were processed with ZEN software. The primary antibodies used were anti-dsRNA 1:200 (kindly donated by Dr. Mariano Garcia-Blanco), anti-NS4A 1:200 (Genetex, GTX124249). The secondary antibodies used were Alexa Fluor 488 conjugated monkey anti-mouse IgG 1:500 (Invitrogen) and Alexa Fluor 555 conjugated donkey anti-rabbit IgG 1:500 (Invitrogen).

2.9. Flow cytometry for viral infection analysis

Cells were fixed with 2% PFA for 20 min, permeabilized and blocked for 20 min with PermWash solution and were incubated with the primary antibody 2H2 or 4G2 overnight at 4 °C. Next, cells were incubated with the secondary antibody coupled to Alexa 488 for 2 h at RT. Flow cytometry was performed in a BD LSR Fortessa quantifying 10,000 events and data were analyzed with FlowJo V.10 Software.

2.10. Cell cycle analysis

For cell cycle analysis, 1×10^7 Huh-7 cells were harvested and wash with PBS 1X, later were fixed with methanol and suspend in 1 ml of the propidium iodide/RNase A staining buffer, and incubated for 10 min at RT. Finally, flow cytometry was performed in a BD LSR Fortessa quantifying 1×10^6 events and data were analyzed with FlowJo V.10 Software.

2.11. siRNA mediated knockdown of Aurora kinase B protein in Huh-7 cells

For siRNA-mediated knockdown of AurKB expression, transfection was carried out using the ambion® silencer siRNA designed for AurKB. The siRNA was transfected by electroporation using the Gene Pulser Xcell (BioRad, Germany). Briefly, a confluent monolayer of Huh-7 cells from p100 plate was harvested and washed with PBS 1X, resuspended in 200 µl of OptiMem medium with 150 nM of AurKB siRNA, and transferred to a Gene Pulse cuvette with 4 mm electrode Gap. An electric field strength and pulse of 170 V for 40 msec in exponential decay was used for electroporation. After the pulse, the cells were plated in p100 plate and incubated at 37 °C with 8 ml of advance DMEM

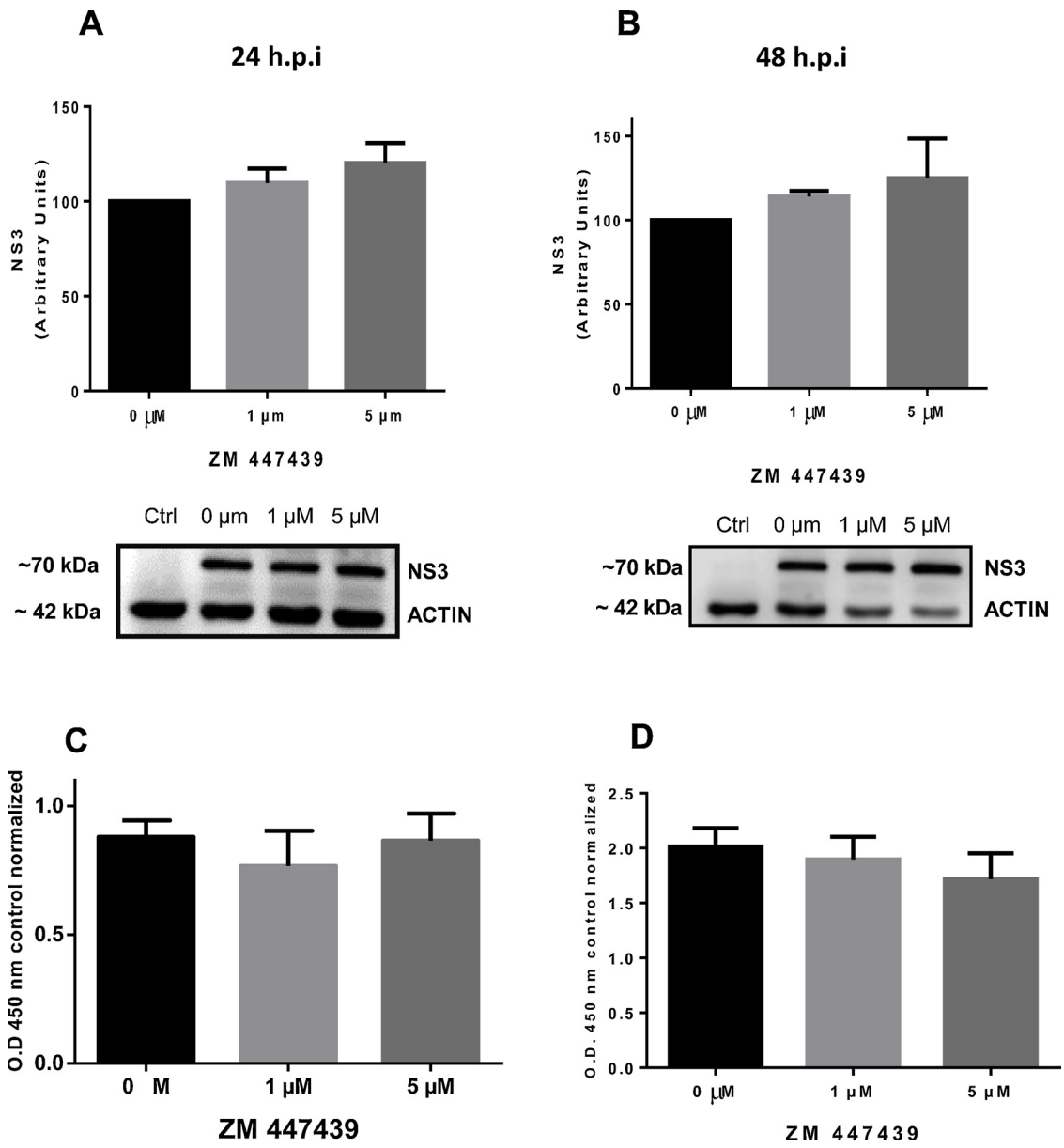

Fig. 3. Effect of ZM 447439 in viral translation. Protein extracts from Huh-7 cells infected at MOI of 3 treated with 1 µM and 5 µm of ZM 447439 for 24 (A) or 48 h (B) were separated by SDS-PAGE and analyzed by Western-blot assay using anti-NS3 antibodies. Actin was used as a loading control. Supernatants of Huh-7 cells infected at MOI of 3 treated with 1 µM and 5 µm of ZM 447439 for 24 (C) or 48 h (D) were used to detect the secreted NS1 protein by Platelia Dengue NS1 (Bio-Rad). Graphs show mean ± SEM of three independent experiments. $*p < 0.05$.

for 4 h. Later, the medium was aspirated and replaced with 10 ml of free medium contain 15% of fetal bovine serum. Twenty hours post transfection, the cells were infected with DENV 2 at M.O.I. of three for 24 h. Finally, the AurKB protein levels were analyzed by Western blot analysis and viral yield was determined from the supernatant of infected cells.

2.12. Statistics analysis

The differences between the diverse treatments and control groups were evaluated using the statistical program GraphPad Prism 6 in all cases. The One tail analysis of variance (ANOVA) was also used. For all tests, a $p \leq 0.05$ was considered statistically significant.

2.13. Ethics statement

This study was conducted in accordance with the official Mexican Standar guidelines for production, care and use of laboratory animals (NOM-062-ZOO-1999) and the protocol number 048-02 was approved by the animal care and use committee (CICUAL) at CINVESTAV-IPN, Mexico City.

3. Results

3.1. AurKB inhibition inhibited the viral particle production but not the percentage of infected cells

Given the important roles of kinases in many cellular functions, we analyzed the relevance of AurKB in the replicative cycle of DENV using the compound ZM 447439, a potent and selective AurKB inhibitor. Initially, the toxicity of the inhibitor was evaluated in Huh-7 cells. The cells were incubated with different concentrations of ZM 447439 (5 and 10 µM) and cell metabolism and viability were determined by MTS reduction and propidium iodide uptake respectively **(**Fig. 1**A and B)**.

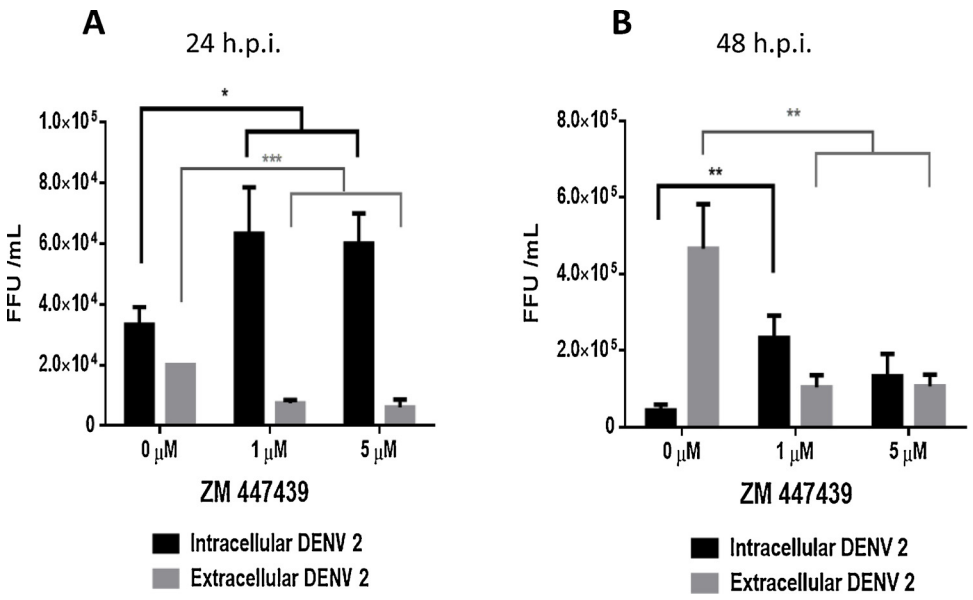

Fig. 4. ZM 447439 inhibits viral yield. Viral yield from supernatant (extracellular) and cell associated (intracellular) obtained at 24 (A) or 48 h.p.i. (B) from Huh-7 cells infected at MOI of 3 treated with 1 μM and 5 μm of ZM 447439 were determined by forming focus assay. Viral yield is expressed as mean ± SEM of FFU/ml of three independent experiments. *P < 0.05.

None of the concentrations caused a significant reduction in cell viability (Fig. 1A). Since the inhibitor should be used for up to 48 h, we decided to perform the following experiments with 1 and 5 μM of ZM 447439.

The next step was to demonstrate that the inhibitor, at the concentrations selected, was able to inhibit the AurKB activity. It is well known that the phosphorylation activity of AurKB is required for the phosphorylation of histone H3 at serine 10 (H3S10p). Thus, the levels of H3S10p were analyzed in untreated and treated cells by Western-blot. In the presence of both 1 and 5 μM of ZM 447439 a reduction of the phosphorylation levels of H3S10p of 17% and 68% respectively was observed (Fig. 1C), supporting the idea that the ZM 447439, at both concentrations, inhibited AurKB activity. On the other hand, it has been described that the inhibition of AurKB induces arrest in the G2/M phase of the cell cycle. Thus, to confirm the inhibition of AurKB activity in the presence of the two concentrations of ZM 447439, the number of cells in the different phases of the cell cycle was analyzed by flow cytometry. At both concentrations, 1 and 5 μM, a 51 and 62% of cells respectively were arrested in G2/M phase compared with the 30% of the cells arrested in G2/M phase in untreated cells. Moreover, the number of cells arrested at 1 μM of ZM 447439 was similar to the ones arrested after treatment with nocodazole (50%), a drug used as a positive control (Fig. 1**D and E).** This arrest was further confirmed using a wider range of concentration (0.1, 0.5, 1.0, 1.5, 2, 2.5, 3, 4, 5, 6, 8 and 10 μM) of the inhibitor ZM 447439 at 24 h.p.i. The EC50 was calculated in 2.5 μM (95% Confidence Interval (CI) = 2.459–2.584 μM) (Supplementary material Fig. 1A)

Once we knew that 1 and 5 μM of ZM 447439 were able to inhibit AurKB activity, the effect of this inhibitor at both particular concentrations was evaluated in DENV2 infection in Huh-7. In the cells treated with ZM 447439, the percentage of infected cells (using an anti-E protein antibody-4G2-) at both concentrations, at 24 and 48 h.p.i. was similar in treated compared to untreated cells (Fig. 2**A and B)**. However, a significant increase in the Mean Fluorescence Intensity (MFI) was observed in ZM 447439 treated cells (Fig. 2**C and D)** compared to untreated cells, suggesting that the inhibition of AurKB does not reduce viral infection but increase the accumulation of viral components inside the cells.

To analyze in further detail the specific step in the replicative cycle of DENV inhibited by ZM 447439, the viral protein synthesis was evaluated in untreated and treated cells by Western-blot. The NS3 protein levels were not altered in cells treated with ZM 447439 for 24 and 48 h compared to untreated cells (Fig. 3**A and B)**. Moreover, similar levels of secreted NS1 protein were detected in untreated and treated cells supernatants from 24 and 48 h.p.i (Fig. 3**C and D)**, supporting the idea that the activity of AurKB is not required for viral translation/replication.

Considering that in ZM 447439 treated cells an increase prM/E signal was observed but not in the NS1 and NS3 proteins levels, it was possible that the new viral particle formation or release could be inhibited avoiding releasing of prM/E in the progeny. Then, the viral titer in the supernatants and in the cell-associated fractions was determined from treated and untreated cells by forming focus assay. In the presence of 1 and 5 μM of ZM 447439 a significant reduction in the viral yield from the supernatant fraction was observed at both 24 (Fig. 4**A)** and 48 h.p.i. (Fig. 4B). In contrast with the significant increase of the viral titer detected in the cell-associated fractions (Fig. 4**A and B)**, suggesting that the inhibition of AurKB impairs viral release.

This inhibition was further confirmed using a wider range of concentration (0.1, 0.5, 1.0, 1.5, 2, 2.5, 3, 4, 5, 6, 8 and 10 μM) of the inhibitor ZM 447439 at 24 h.p.i. The EC50 was calculated in 3.8 μM (95% CI = 2.851–5.064 μM). (Supplementary material Fig. 1B)

3.2. ZM 447439 treatment alters RCs distribution

Since DENV morphogenesis takes place in a close proximity to the RC, we analyzed distribution of these components after treatment with ZM 447439. The location and distribution of the dsRNA and the non-structural protein 4A (NS4A), markers of the RC, were analyzed by confocal microscopy. As expected, a perinuclear distribution of dsRNA and NS4A with a co-localization index of 0.42 was observed in untreated cells. Interestingly, when cells were treated with 1 and 5 μM of ZM 447439 the co-localization between dsRNA and NS4A was reduced (co-localization = 0.19 and 0.20 respectively) (Fig. 5**A and B)**, suggesting that the inhibition of AurKB alters not only viral release but also the correct RC formation.

3.3. Silencing of AurKB induces a decrease in viral yield

To further confirm the role of AurkB in viral morphogenesis/release, silencing of the kinase was performed using a specific siRNA directed to knockdown AurKB and the viral yield present in the supernatant of transfected cells was evaluated by plaque assay. The significant reduction in AurkB protein levels detected in silenced cells (61%) (Fig. 6**A and B**) caused a significant decrease in the viral yield compared with cells transfected with the unrelated siRNA (1 log or 96%) (Fig. 6C),

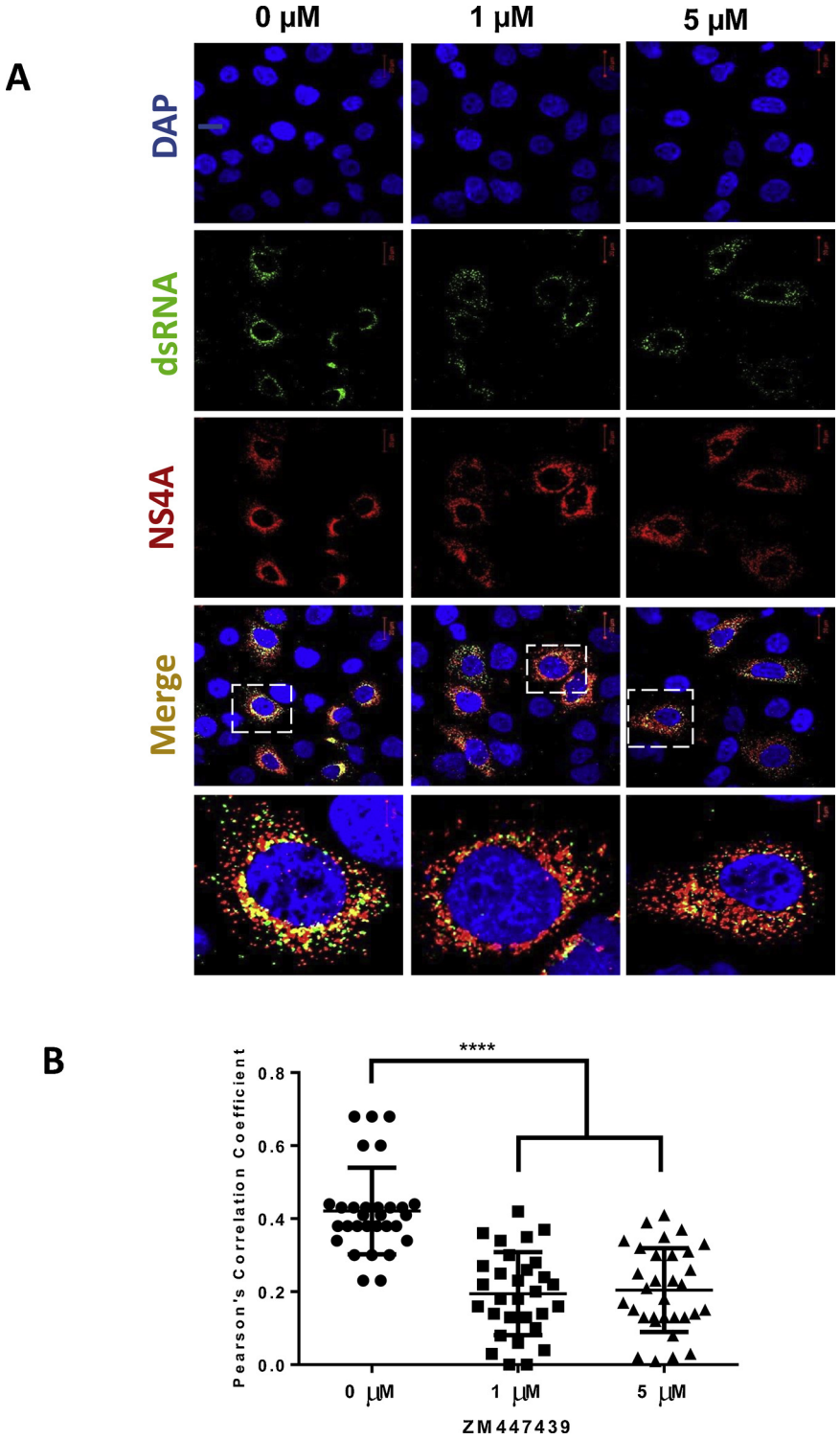

Fig. 5. ZM 447439 alters the colocalization of NS4A and dsRNA. Cells infected with DENV 2 at a MOI of 3 treated with vehicle, 1 μM or 5 μM of ZM 447439 for 24 h were fixed and incubated with anti-dsRNA (green) and anti-NS4A antibodies (Red). Nuclei were counterstained with DAPI (Blue). Distribution pattern of viral proteins was analyzed by confocal microscopy (A). Selected area (white box) was amplified showing the localization of viral components. Colocalization index between NS4A and dsRNA is shown (B). ****$p < 0.0001$. Representative images of three independent experiments are presented.

confirming the role of AurkB in viral morphogenesis/release.

4. Discussion

DENV is an important re-emergent arboviral disease in the world. Recent estimation indicates that 390 million persons per year are infected with DENV and almost 96 million are symptomatic patients (Bhatt, Gething et al. 2013). The presence of mosquito vector in broad regions and the co-circulation of two or more serotypes in the same area increase viral dispersion to non-endemic regions. All these elements in combination with the lack of a highly protective vaccine against DENV infection and the absence of an effective antiviral treatment have made of this infection an important world health challenge, highlighting the importance to develop new control strategies, including surveillance

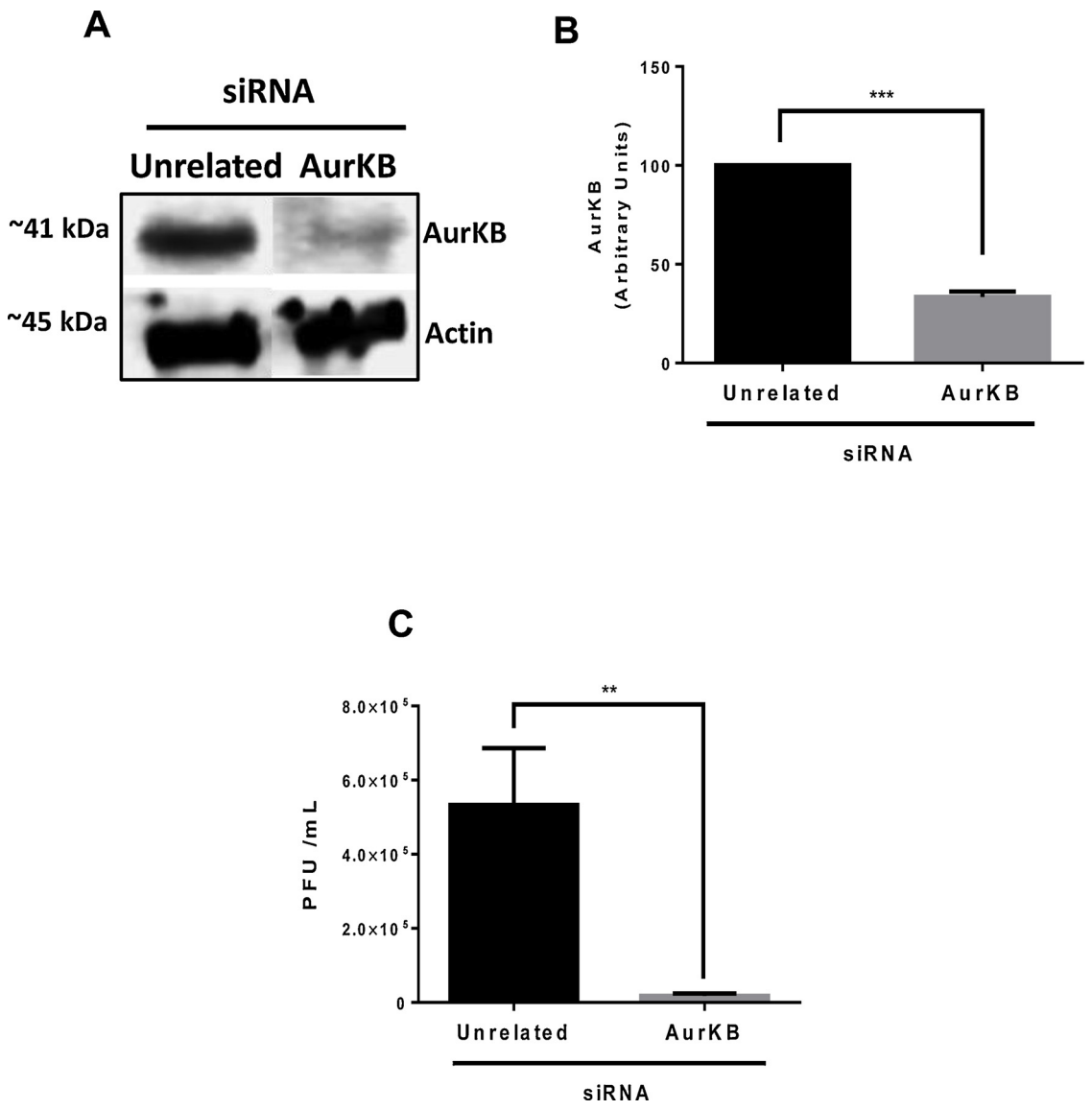

Fig. 6. Knockdown of AurKB reduces viral yield. Huh-7 cells were transfected with specific AurKB siRNA for 24 h and the kinase protein level was evaluated by Western-blot (A). Actin was used as a loading control. Densitometric analysis of AurKB silencing (B). Graph shows mean ± SEM of three independent experiments. $^{*}p < 0.05$. The Huh-7 cells transfected with specific AurKB siRNA for 24 h were infected with DENV 2 at a MOI of 3 for 24 h. The supernatants were collected, and viral yield was determined by plaque assay (C). Data are means ± standard error (S.E) of three independent experiments. $^{**}p < 0.01$ and $^{***}p < 0.01$.

and the design and development of an effective therapy against DENV.

The protein phosphorylation is the most common and important post-translational modification (PTM) which regulates several essential functions of the cells such as, protein synthesis, cell growth and division, signal transduction, and transcription, among many other process related to cellular metabolism (Ubersax and Ferrell, 2007). Actually, it is well known that up to 30% of human proteins can be phosphorylated (Ardito, Giuliani et al. 2017). This PTM is regulated by two kinds of enzymes, the kinases and the phosphatases. The protein kinases can be divided in two different classes, the serine/threonine kinases and the tyrosine kinases (Roskoski, 2012). Protein phosphorylation by kinases can regulate the protein function through two mechanisms, inducing conformational changes or creating protein-protein interaction surfaces in the substrate (Serber and Ferrell, 2007; Holt, Tuch et al. 2009).

During flavivirus replicative cycle, kinases play an important role participating in different steps such as, entry, translation, genome replication, assembly, and release (Anwar, Hosoya et al. 2011; Madejon, Sheldon et al. 2015; Noppakunmongkolchai, Poyomtip et al. 2016; Bekerman, Neveu et al. 2017; Limjindaporn, Panaampon et al. 2017). Moreover, it has been reported that kinases can phosphorylate flavivirus polymerase NS5 regulating its function and sub-cellular localization (Forwood, Brooks et al. 1999; Bhattacharya et al., 2009). Thus, the kinases inhibition is a promising strategy against flavivirus and other emergent virus infection such as Ebola (Bekerman, Neveu et al. 2017).

In this report, we analyzed the role of Aurora Kinase B in DENV replicative cycle. AurKB is called the “master regulator of cell cycle” because its function is regulated during the G2/M and cytokinesis of the cell cycle (Fu, Bian et al. 2007). We analyzed the role of AurKB in DENV by using the specific inhibitor ZM 447439. The main effect of the drug was a reduction in viral yield from the supernatant fraction, but not in the viral yield from the cell-associated fraction or the number of infected cells, indicating that viral release is altered. This result is in accordance with our results that demonstrate that in the presence of the ZM 447439 inhibitor, viral translation and replication were not modified and with the fact that the silencing of AurkB inhibited the viral yield in the supernatant of infected and knockdown cells. To this regard, the discrete loss of NS4A and dsRNA colocalization might not be related with an altered RC function but could be associated with an

impaired route for viral release through the ER membranes.

Similar results of a decolocalization of some viral components and the inhibition of viral assembly were obtained previously when the kinases inhibitor SFV785 was used in DENV infected cells (Anwar, Hosoya et al. 2011). While the SFV785 is an inhibitor of several kinases such as TrkA (*Tropomyosin receptor kinase*) and MAPKAPK5 (*MAPK-activated protein kinase 5*), the inhibitor that we used, the ZM 447439 is a specific inhibitor of AurKB.

It has been described that AurKB phosphorylates vimentin, and causes a dramatical inhibition of vimentin filament formation and an alteration in the rearrangement of the filaments (Goto, Yasui et al. 2003). Moreover, the phosphorylation of vimentin regulates its binding with other proteins (Tzivion, Luo et al. 2000); thus, it is possible that the inhibition of AurKB activity alters vimentin phosphorylation, polymerization or binding to other proteins. The role of vimentin in RC formation during DENV infection through its direct interaction with NS4A has been described (Teo and Chu, 2014). It has also been observed that vimentin interacts with the DENV non-structural protein 1 (NS1) playing a role in the release of viral progeny (Kanlaya, Pattanakitsakul et al. 2010). Thus, the inhibition of AurKB could alter RCs formation impairing viral budding or release.

Additionally, AurKB phosphorylates CHMP4C during cytokinesis (Carlton, Caballe et al. 2012). Phosphorylation of CHMP4C is an essential step for ESCRT-III complex assembly. This complex is involved in flavivirus particle formation and viral budding from ER (Tabata, Arimoto et al. 2016). Thus, if CHMP4C phosphorylation is inhibited by ZM 447439 the viral assembly or budding from ER to Golgi cisternae should be inhibited.

In summary, our data describe the importance of AurKB in DENV 2 release from the infected cells and suggest a role of this protein in the budding of the viruses through the ER. Further studies are required to identify the cellular or viral components primary altered by the presence of the inhibitor ZM 447439 or the silencing of the kinase. Additionally, our results support the idea that AurKB can be a suitable target for antiviral design.

Declaration of Competing Interest

The authors declare that they have no competing interest.

Acknowledgement

This work was funded by the National Council of Science and Technology of Mexico (CONACyT) Grant 417968. Jose Humberto Perez Olais had a scholarship from CONACyT. We thank to Dr. Ana Lorena Gutierrez Escolano for critical review of manuscript, Diego Soto-Cabrera and Jaime Zarco for technical assistance, Fernando Medina-Ramírez for the maintenance of cell lines and mice.

Appendix A. Supplementary data

Supplementary material related to this article can be found, in the online version, at doi:https://doi.org/10.1016/j.virusres.2019.197777.

References

Anwar, A., Hosoya, T., Leong, K.M., Onogi, H., Okuno, Y., Hiramatsu, T., Koyama, H., Suzuki, M., Hagiwara, M., Garcia-Blanco, M.A., 2011. The kinase inhibitor SFV785 dislocates dengue virus envelope protein from the replication complex and blocks virus assembly. PLoS One 6 (8), e23246.

Ardito, F., Giuliani, M., Perrone, D., Troiano, G., Lo Muzio, L., 2017. The crucial role of protein phosphorylation in cell signaling and its use as targeted therapy (Review). Int. J. Mol. Med. 40 (2), 271–280.

Bekerman, E., Neveu, G., Shulla, A., Brannan, J., Pu, S.Y., Wang, S., Xiao, F., Barouch-Bentov, R., Bakken, R.R., Mateo, R., Govero, J., Nagamine, C.M., Diamond, M.S., De Jonghe, S., Herdewijn, P., Dye, J.M., Randall, G., Einav, S., 2017. Anticancer kinase inhibitors impair intracellular viral trafficking and exert broad-spectrum antiviral effects. J. Clin. Invest. 127 (4), 1338–1352.

Bhatt, S., Gething, P.W., Brady, O.J., Messina, J.P., Farlow, A.W., Moyes, C.L., Drake, J.M., Brownstein, J.S., Hoen, A.G., Sankoh, O., Myers, M.F., George, D.B., Jaenisch, T., Wint, G.R., Simmons, C.P., Scott, T.W., Farrar, J.J., Hay, S.I., 2013. The global distribution and burden of dengue. Nature 496 (7446), 504–507.

Bhattacharya, D., Ansari, I.H., Striker, R., 2009. The flaviviral methyltransferase is a substrate of Casein Kinase 1. Virus Res. 141 (1), 101–104.

Carlton, J.G., Caballe, A., Agromayor, M., Kloc, M., Martin-Serrano, J., 2012. ESCRT-III governs the Aurora B-mediated abscission checkpoint through CHMP4C. Science 336 (6078), 220–225.

Carmena, M., Wheelock, M., Funabiki, H., Earnshaw, W.C., 2012. The chromosomal passenger complex (CPC): from easy rider to the godfather of mitosis. Nat. Rev. Mol. Cell Biol. 13 (12), 789–803.

Forwood, J.K., Brooks, A., Briggs, L.J., Xiao, C.Y., Jans, D.A., Vasudevan, S.G., 1999. The 37-amino-acid interdomain of dengue virus NS5 protein contains a functional NLS and inhibitory CK2 site. Biochem. Biophys. Res. Commun. 257 (3), 731–737.

Fu, J., Bian, M., Jiang, Q., Zhang, C., 2007. Roles of Aurora kinases in mitosis and tumorigenesis. Mol. Cancer Res. 5 (1), 1–10.

Georgieva, I., Koychev, D., Wang, Y., Holstein, J., Hopfenmuller, W., Zeitz, M., Grabowski, P., 2010. ZM 447439, a novel promising aurora kinase inhibitor, provokes antiproliferative and proapoptotic effects alone and in combination with bio- and chemotherapeutic agents in gastroenteropancreatic neuroendocrine tumor cell lines. Neuroendocrinology 91 (2), 121–130.

Goto, H., Yasui, Y., Kawajiri, A., Nigg, E.A., Terada, Y., Tatsuka, M., Nagata, K., Inagaki, M., 2003. Aurora-B regulates the cleavage furrow-specific vimentin phosphorylation in the cytokinetic process. J. Biol. Chem. 278 (10), 8526–8530.

Harak, C., Lohmann, V., 2015. Ultrastructure of the replication sites of positive-strand RNA viruses. Virology 479-480, 418–433.

Holt, L.J., Tuch, B.B., Villen, J., Johnson, A.D., Gygi, S.P., Morgan, D.O., 2009. Global analysis of Cdk1 substrate phosphorylation sites provides insights into evolution. Science 325 (5948), 1682–1686.

Hu, Y., Zhang, J., Musharrafieh, R., Hau, R., Ma, C., Wang, J., 2017. Chemical Genomics Approach Leads to the Identification of Hesperadin, an Aurora B Kinase Inhibitor, as a Broad-Spectrum Influenza Antiviral. Int. J. Mol. Sci. 18 (9).

Jha, H.C., Lu, J., Saha, A., Cai, Q., Banerjee, S., Prasad, M.A., Robertson, E.S., 2013. EBNA3C-mediated regulation of aurora kinase B contributes to Epstein-Barr virus-induced B-cell proliferation through modulation of the activities of the retinoblastoma protein and apoptotic caspases. J. Virol. 87 (22), 12121–12138.

Jha, H.C., Yang, K., El-Naccache, D.W., Sun, Z., Robertson, E.S., 2015. EBNA3C regulates p53 through induction of Aurora kinase B. Oncotarget 6 (8), 5788–5803.

Jordan, T.X., Randall, G., 2017. Dengue virus activates the AMP Kinase-mTOR Axis To stimulate a proviral lipophagy. J. Virol. 91 (11).

Kanlaya, R., Pattanakitsakul, S.N., Sinchaikul, S., Chen, S.T., Thongboonkerd, V., 2010. Vimentin interacts with heterogeneous nuclear ribonucleoproteins and dengue nonstructural protein 1 and is important for viral replication and release. Mol. Biosyst. 6 (5), 795–806.

Keating, J.A., Bhattacharya, D., Rund, S.S., Hoover, S., Dasgupta, R., Lee, S.J., Duffield, G.E., Striker, R., 2013. Mosquito protein kinase G phosphorylates flavivirus NS5 and alters flight behavior in Aedes aegypti and Anopheles gambiae. Vector Borne Zoonotic Dis. 13 (8), 590–600.

Kovackova, S., Chang, L., Bekerman, E., Neveu, G., Barouch-Bentov, R., Chaikuad, A., Heroven, C., Sala, M., De Jonghe, S., Knapp, S., Einav, S., Herdewijn, P., 2015. Selective inhibitors of cyclin g associated kinase (GAK) as anti-hepatitis C agents. J. Med. Chem. 58 (8), 3393–3410.

Limjindaporn, T., Panaampon, J., Malakar, S., Noisakran, S., Yenchitsomanus, P.T., 2017. Tyrosine kinase/phosphatase inhibitors decrease dengue virus production in HepG2 cells. Biochem. Biophys. Res. Commun. 483 (1), 58–63.

Lindenbach, B.D., Rice, C.M., 2003. Molecular biology of flaviviruses. Adv. Virus Res. 59, 23–61.

Madejon, A., Sheldon, J., Francisco-Recuero, I., Perales, C., Dominguez-Beato, M., Lasa, M., Sanchez-Perez, I., Muntane, J., Domingo, E., Garcia-Samaniego, J., Sanchez-Pacheco, A., 2015. Hepatitis C virus-mediated Aurora B kinase inhibition modulates inflammatory pathway and viral infectivity. J. Hepatol. 63 (2), 312–319.

Miller, S., Sparacio, S., Bartenschlager, R., 2006. Subcellular localization and membrane topology of the Dengue virus type 2 Non-structural protein 4B. J. Biol. Chem. 281 (13), 8854–8863.

Murray, J.M., Aaskov, J.G., Wright, P.J., 1993. Processing of the dengue virus type 2 proteins prM and C-prM. J. Gen. Virol. 74 (Pt 2), 175–182.

Noppakunmongkolchai, W., Poyomtip, T., Jittawuttipoka, T., Luplertlop, N., Sakuntabhai, A., Chimnaronk, S., Jirawatnotai, S., Tohtong, R., 2016. Inhibition of protein kinase C promotes dengue virus replication. Virol. J. 13, 35.

Roskoski Jr., R., 2012. ERK1/2 MAP kinases: structure, function, and regulation. Pharmacol. Res. 66 (2), 105–143.

Sanofi, 2017. Sanofi Updates Information on Dengue Vaccine Sanofi. Paris, France. .

Serber, Z., Ferrell Jr., J.E., 2007. Tuning bulk electrostatics to regulate protein function. Cell 128 (3), 441–444.

Suwonkerd, W., Mongkalangoon, P., Parbaripai, A., Grieco, J., Achee, N., Roberts, D., Chareonviriyaphap, T., 2006. The effect of host type on movement patterns of Aedes aegypti (Diptera: culicidae) into and out of experimental huts in Thailand. J. Vector Ecol. 31 (2), 311–318.

Tabata, K., Arimoto, M., Arakawa, M., Nara, A., Saito, K., Omori, H., Arai, A., Ishikawa, T., Konishi, E., Suzuki, R., Matsuura, Y., Morita, E., 2016. Unique requirement for ESCRT factors in flavivirus particle formation on the endoplasmic reticulum. Cell Rep. 16 (9), 2339–2347.

Teo, C.S., Chu, J.J., 2014. Cellular vimentin regulates construction of dengue virus replication complexes through interaction with NS4A protein. J. Virol. 88 (4), 1897–1913.

Tzivion, G., Luo, Z.J., Avruch, J., 2000. Calyculin A-induced vimentin phosphorylation sequesters 14-3-3 and displaces other 14-3-3 partners in vivo. J. Biol. Chem. 275 (38), 29772–29778.
Ubersax, J.A., Ferrell Jr., J.E., 2007. Mechanisms of specificity in protein phosphorylation. Nat. Rev. Mol. Cell Biol. 8 (7), 530–541.
Welsch, S., Miller, S., Romero-Brey, I., Merz, A., Bleck, C.K., Walther, P., Fuller, S.D., Antony, C., Krijnse-Locker, J., Bartenschlager, R., 2009. Composition and three-dimensional architecture of the dengue virus replication and assembly sites. Cell Host Microbe 5 (4), 365–375.
WHO, 2009. Dengue: Guidelines for Diagnosis, Treatment, Prevention and Control: New Edition. WHO, Geneva, Switzerland.